18F-fluorodeoxyglucose positron emission tomography/computed tomography findings of breast cancer with signet ring cell differentiation: A single-center experience

Taşlı yüzük hücre diferansiye meme kanserinde 18F-florodeoksiglikoz positron emisyon tomografi/bilgisayarlı tomografi bulguları: Tek merkez deneyimi

Goksel Alcin[1], Esra Arslan[1]

[1] University of Health Sciences Turkey, Istanbul Training and Research Hospital, Clinic of Nuclear Medicine

Abstract

Aim: Due to the low incidence of breast cancer with signet ring cell (SRC) differentiation, which constitutes less than 1% of all breast cancers, little is known about its imaging features. The aim of this study was to evaluate the utility of 18F-Fluorodeoxyglucose (18F-FDG) Positron Emission Tomography/Computed Tomography (PET/CT) in staging breast cancer with SRC differentiation.

Methods: We conducted a retrospective analysis of 14 patients with histologically confirmed breast cancer with SRC differentiation who underwent 18F-FDG PET/CT at our institution between 2014 and 2023. The imaging findings were analyzed in terms of maximum standardized uptake value (SUVmax), lesion size, and the presence of regional or distant metastases were statistically evaluated.

Results: The histological subtypes of SRC differentiated primary tumors were 9 invasive lobular, and 5 invasive ductal carcinoma. More intense 18F-FDG uptake was observed in primary tumoral lesions of the ductal subtype (mean SUVmax: 18.8±9.8; range: 2.6–28.9) compared to the lobular subtype (mean SUVmax: 2.6±1.3; range: 1.5–5.1) (p=0.007, Z=2.600). Among the patients included in the study, axillary lymph node metastasis was present in 64% (n=9) of the cases, with lymph node metastasis identified in five cases classified as ductal carcinoma. Additionally, distant organ metastasis was identified in 21% (n=3) of patients, comprising two patients with ductal carcinoma and one with lobular carcinoma.

Conclusion: Despite the general consensus that signet-ring cell tumors have a low affinity for 18F-FDG, our study has observed the possibility of high 18F-FDG uptake in cases of ductal carcinoma. However, in cases of lobular carcinoma, where 18F-FDG uptake tends to be low, considering alternative PET radiopharmaceuticals for imaging could be a viable option.

Keywords: Breast cancer; F18-fluorodeoxyglucose; positron emission tomography computed tomography; signet ring cell carcinoma

Öz

Amaç: Tüm meme kanserlerinin %1'inden daha azını oluşturan taşlı yüzük hücre diferansiye meme kanseri vakalarının nadir görülmesi nedeniyle, görüntüleme özellikleri hakkında sınırlı bilgi bulunmaktadır. Bu çalışmanın amacı, taşlı yüzük hücreli diferansiye meme kanserinin evrelemesinde 18F-FDG PET/BT'nin yararlılığını değerlendirmektir.

Yöntemler: 2014 ile 2023 yılları arasında kurumumuzda 18F-FDG PET/BT yapılan, histopatolojik olarak teyit edilmiş taşlı yüzük hücreli diferansiye meme kanseri tanısı alan 14 hasta üzerinde retrospektif bir analiz gerçekleştirdik. Görüntüleme bulguları, maksimum standartlaştırılmış uptake değeri (SUVmax), lezyon boyutu ve bölgesel veya uzak metastaz varlığı istatistiksel olarak incelendi.

Bulgular: Taşlı yüzük hücreli diferansiye primer tümörlerin histolojik alt tipleri, 9 invaziv lobüler ve 5 invaziv duktal karsinomdu. Primer tümör lezyonlarında duktal alt tipin (ortalama SUVmax: 18.8±9.8; aralık: 2.6–28.9) lobüler alt tip (ortalama SUVmax: 2.6±1.3; aralık: 1.5–5.1) ile karşılaştırıldığında daha yoğun 18F-FDG tutulumu gösterdiği saptandı (p=0.007, Z=2.600). Çalışmaya dahil edilen hastalar arasında, vakaların %64'ünde (n=9) aksiller lenf nodu metastazı bulunurken, duktal karsinom olarak sınıflandırılan beş vakada lenf nodu metastazı saptandı. Ayrıca, hastaların %21'inde (n:3) uzak organ metastazı tespit edildi; bunların ikisi duktal karsinom ve biri lobüler karsinom idi.

Sonuç: Taşlı yüzük hücreli tümörlerin 18F-FDG'ye düşük affinitesi olduğu genel kabul görmesine rağmen, çalışmamız duktal karsinomlu olgularda yüksek 18F-FDG tutulumu olabileceği gözlemlemiştir. Lobüler karsinomlu olgularda ise 18F-FDG tutulumunun düşük olması nedeniyle, diğer PET radyofarmasötikleri ile görüntüleme seçenekleri düşünülebilir.

Anahtar Sözcükler: F18-fluorodeoksiglukoz, meme kanseri, pozitron emisyon tomografi bilgisayarlı tomografi, taşlı yüzük hücreli karsinom

Received/*Geliş* : 11.08.2023
Accepted/*Kabul*: 03.09.2023

DOI: 10.21673/anadoluklin.1341711

Corresponding author/*Yazışma yazarı*
Göksel Alçın
Sağlık Bilimleri Üniversitesi, İstanbul Eğitim ve Araştırma Hastanesi, Nükleer Tıp Kliniği, İstanbul, Türkiye
E-mail: drgokselalcin@hotmail.com

ORCID
Göksel Alçın: 0000-0003-2268-9606
Esra Arslan: 0000-0002-9222-8883

INTRODUCTION

Breast cancer is the most common cancer in women worldwide and has a variety of histological subtypes (1). Miscellaneous histological and immuno-molecular studies have revealed the inherent heterogeneity of breast cancer, emphasizing its diverse nature (2,3). Signet ring cell (SRC) is a type of malignant cell with abundant intracytoplasmic mucin, imparting a signet ring appearance. When SRCs comprise the primary component of a tumor, it is classified as signet ring cell carcinoma (SRCC), commonly observed in gastrointestinal carcinomas. This particular subtype has been linked to a poorer prognosis compared to other cancer subtypes (4).

The definition of primary invasive SRCC of the breast has shown variation among the limited number of published series available. The presence of SRCs in breast cancer was first described by Saphir (5). Initially, it was believed that SRCs in breast tumors primarily originated from invasive lobular carcinoma (ILC). However, subsequent studies have revealed that SRCs can also arise from other types of carcinoma, such as invasive ductal carcinoma of no special type (IDC-NST) and mucinous carcinoma (MC) (3,6,7). SRCC was classified under the category of mucin-producing carcinomas by the World Health Organization (WHO) until 2003 and was distinguished from infiltrating ductal and lobular carcinomas. In the Fourth Edition of the WHO Classification of Breast Tumors (2012), SRCC was revised to breast cancer with SRC differentiation, signifying the acknowledgment that this particular subtype no longer retains an independent categorization (2,8).

In daily clinical practice, breast carcinomas with SRC differentiation are rare, and the role of 18F-Fluorodeoxyglucose (18F-FDG) Positron Emission Tomography/Computed Tomography (PET/CT) in the staging and patient management of this breast cancer subtype is not well defined. (4,9). The aim of this study is to assess the utility of 18F-FDG PET/CT in staging differentiated breast cancer with SRC differentiation.

MATERIALS AND METHODS

Patient Selection and Evaluation

A total of 1765 patients diagnosed with breast cancer who underwent 18F-FDG PET/CT for staging at our institution between September 2014 and February 2023 were retrospectively evaluated. Fourteen patients (0.79%) with histopathologically confirmed SRC differentiated breast cancer were enrolled in this study (Figure 1).

This study was conducted under the Declaration of Helsinki. This study was approved by University of Health Sciences Turkey, Istanbul Training and Research Hospital Clinical Research Ethics Committee (Date: 12.05.2023, Decision no: 121) and written informed consent was obtained from all participants.

PET/CT Imaging and Evaluation

The administered doses of radiopharmaceuticals (0.1 mCi/kg for 18F-FDG) were calculated based on the patient's weight. Sixty minutes after the intravenous injection, vertex-upper thigh imaging was performed, and additional imaging of the lower extremities was conducted if necessary. All patient data were acquired using a high-resolution PET/CT device (Biograph mCT 20; Siemens Molecular Imaging, Hoffman Estates, IL).

A thorough reassessment of all images was conducted by board-certified nuclear medicine physicians with a minimum of ten years of experience in PET/CT. In addition to visual assessment, the SUVmax was determined by delineating volumes of interest (VOIs) in the primary tumor, lymph nodes, skeleton, and other anatomical regions with higher uptake than background activity on 18F-FDG PET/CT. Furthermore, the size of the primary breast and metastatic lesions were documented, and additional evaluations at the patient and lesion levels were performed.

Histological Analysis

Histopathological analysis of primary breast cancer was conducted using fine needle aspiration biopsy (FNAB) or tru-cut biopsy of the primary tumor, guided by ultrasound (USG) or mammography images, or through breast surgery/excisional biopsy following 18F-FDG PET/CT imaging. Patients with an SRC percentage of 20% or more in tumor sections were included in the study. Based on their immunohistochemical (IHC) results, the patients were divided into four subgroups (Luminal A-B, HER-2, and TNBC). The axillary metastases indicated on PET/CT were histopathologically

Table 1. Patient characteristics

Variables	**n, %**
Histologic subtype	
IDC	5 (35.7%)
ILC	9 (64.3%)
Molecular subtype	
Luminal A	6 (42.9%)
Luminal B	7 (50.0%)
HER2-positive	1 (7.1%)
Triple-negative	-
Menopause status	
Pre-/Post-	2 / 12
Family history	
+/–	4 / 10
Primary tumor localization	
Right/Left	4 / 10
ER status	
+/–	13 / 1
PR status	
+/–	12 / 2
HER2 status	
+/–	4 / 10
Median (minimum-maximum)	
Ki-67 (%)	20 (4–65)
Age (years)	58 (44–71)
Follow-up (months)	62 (4–107)
Status	
Dead/alive	2/12

* IDC: Invasive ductal cancer, ILC: Invasive lobular cancer, ER: Estrogen receptor, PR: Progesterone receptor, HER2: Human Epidermal Growth Factor receptor, n: number, %: percent.

verified. In one case diagnosed with an ovarian mass, IHC markers (CK7, CK20, PAX8, CDX2, GATA3, Mamoglobin, ER, PR, MUC2, Synaptophysin, and Chromogranin) were utilized for determining the primary tumor localization

Statistical analysis

All statistical analyses were conducted using Statistical Package for the Social Sciences (IBM SPSS Statistics for Mac, version 25.0; Armonk, New York, USA). The normality analysis was assessed using the Shapiro-Wilk test. Descriptive statistics, including mean, standard deviation, minimum, median, and maximum, were utilized to summarize continuous variables. Mann-Whitney U or Spearman's rho tests were used to analyze SUVmax measurements from primary tumor lesions and metastases on 18F-FDG PET/CT. Kaplan-Meier method was employed for survival analysis. Statistical significance was considered at a p-value of less than 0.05.

RESULTS

The median age of the patients was 58 (44–71). Twelve patients (85.7%) were postmenopausal, and four (28.5%) had a family history of breast cancer. Histological subtypes comprised nine lobular and five invasive ductal patients. In 13 patients (92.8%), estrogen receptor (ER) positivity was detected, while 12 patients (85.7%) showed positivity for progesterone receptor (PR). Also, four patients (28.5%) were HER-2 positive. The mean Ki-67% score was 20 (4–65). Six patients (42.9%) were Luminal A, seven patients (50.0%) were Luminal B, and one patient (7.1%) was HER2-positive.

Table 2. Clinical / Histopathological characteristics of patients

Patient	Age	Tumor Site	Histologic Subtype	Molecular Subtype	Nuclear Grade	Ki 67%	Estrogen Receptor Score	Estrogen Receptor Percentage %	Progesteron Receptor Score	Progesteron Receptor Percentage %	HER-2 Score / IHC Result	Follow-up (months)	Status
01.	71	Right	Lobular	Luminal B	2	35	+++	100	+++	90	–	80	Alive
02.	59	Left	Ductal	HER-2 type	3	55	–	0	–	0	+++/+	57	Alive
03.	52	Left	Lobular	Luminal A	2	10	+++	100	+++	100	–	86	Alive
04.	60	Left	Lobular	Luminal A	2–3	10	+++	95	+++	95	–	69	Alive
05.	60	Left	Lobular	Luminal B	2	30	+++	100	+	5	++/+	98	Alive
06.	45	Left	Lobular	Luminal A	2	10	+++	100	+++	100	–	107	Alive
07.	57	Left	Ductal	Luminal B	3	50	+++	100	++	65	–	66	Alive
08.	70	Left	Ductal	Luminal B	3	65	+++	100	+++	60	++/+	35	Dead
09.	55	Left	Lobular	Luminal A	2–3	4	+++	100	+++	100	–	32	Alive
10.	68	Right	Lobular	Luminal B	2	12	+++	100	–	0	–	59	Dead
11.	62	Right	Ductal	Luminal B	2	35	+++	100	+++	70	++/+	24	Alive
12.	50	Left	Lobular	Luminal A	3	10	+++	100	+++	95	–	77	Alive
13.	44	Left	Lobular	Luminal A	2–3	5	+++	95	+++	85	–	6	Alive
14.	52	Right	Ductal	Luminal B	2	29	+++	90	+++	90	–	4	Alive

HER2: Human Epidermal Growth Factor receptor, IHC: Immunohistochemical

Table 3. Characteristics of the primary tumor, and metastases

Patient	Primary Tumor size (mm)	Primary Tumor 18F-FDG SUVmax	Axillary lymph node size (mm)	Axillary lymph node 18F-FDG SUVmax	Extra-axillary lymph node 18F-FDG SUVmax	Bone metastasis 18F-FDG SUVmax	Additional lesions 18F-FDG SUVmax
01.	14	2,5	15	4,7			
02.	50	22,3	10	1,6			
03.	10	2,1	11	1,9			
04.	42	1,6					
05.	25	4,6	20	2,9			
06.	15	2,9					
07.	19	21,4	22	27,6	8,1	17,6	
08.	92	28,9	12	3,4			
09.	22	1,9			8,7	4,5	7,3* / 11,0**
10.	36	1,8					
11.	27	18,7	10	3,4		17,7	
12.	30	5,1	10	2,7			
13.	10	1,5					
14.	65	2,6	12	5,9			

18F-FDG: 18F-Fluorodeoxyglucose, * = over metastasis, ** = peritoneal implant lesions

Breast cancer was detected unilaterally in all patients. No tumors showed multifocality/multicentricity (Table 1–2).

In the patient cohort included in this study, primary tumoral lesions of the ductal subtype (mean:18.8±9.8; 2.6–28.9) exhibited significantly higher 18F-FDG uptake than those of the lobular subtype (mean:2.6±1.3; 1.5–5.1) (p=0.007, Z=2.600) (Table 3). Four patients with ductal carcinoma were classified as Luminal B, and one belonged to the HER-2 group. Among the patients with lobular cancer, six were classified as Luminal A, and three were classified as Luminal B. Additionally, the mean Ki-67% value was 47 in the ductal carcinoma group and 14 in the lobular carcinoma group.

In five patients with lobular carcinoma (55.5%), primary lesions were barely distinguishable from parenchymal background uptake on 18F-FDG PET/

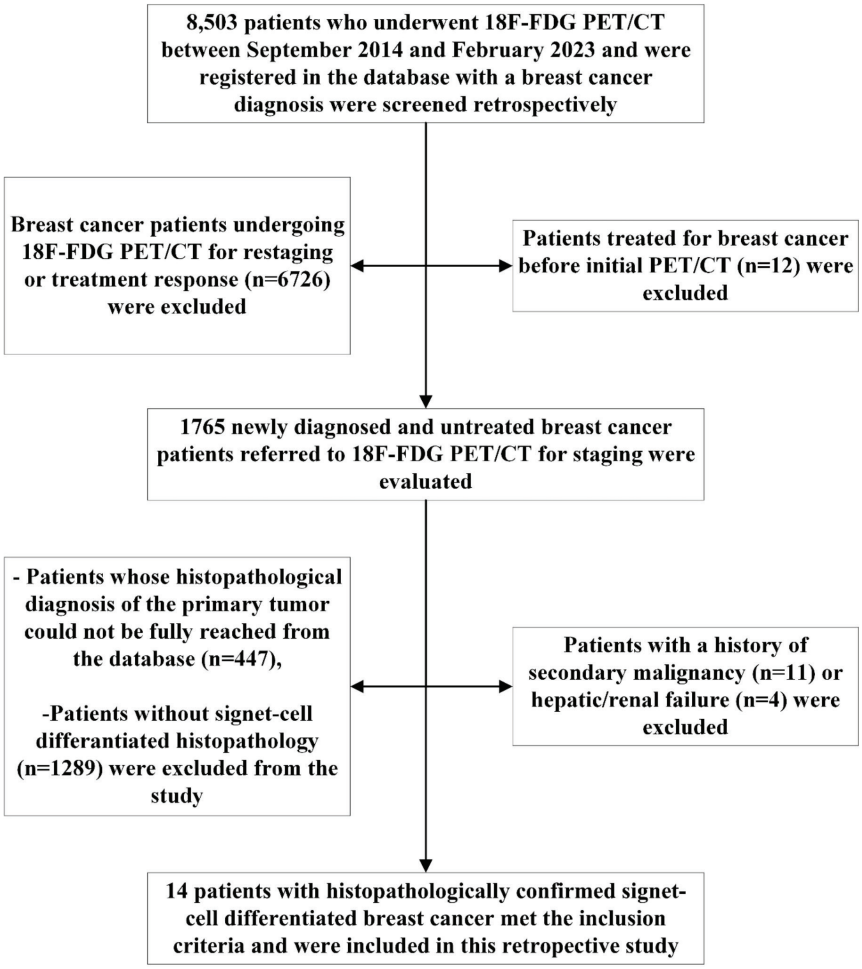

Figure 1. 18F-FDG PET/CT: 18F-Fluorodeoxyglucose Positron Emission Tomography/Computed Tomography

CT. Additional 68Gallium-Fibroblast activation protein inhibitor (68Ga-FAPI) PET/CT scans were also performed on two patients. In the first patient, there was no significant pathological FDG uptake in the breast parenchyma; however, mild 18F-FDG uptakes were detected in dense fibroglandular tissue in both breasts (SUVmax: 3.78). In 68Ga-FAPI PET/CT imaging, the focal uptake of FAPI in the primary breast tumor (SUVmax: 5.9) could be distinctly identified, albeit slightly higher than the background parenchyma (SUVmax: 5,4) (Figure 2). In the other patient, surgery (total abdominal hysterectomy and bilateral salpingo-oophorectomy) was performed due to ovarian masses, and SRCC metastasis diagnosis was established. IHC analysis revealed IHC analysis revealed Cytokeratin 7 (CK) (+), CK 20 (-), PAX8 (-), CDX2 (-), GATA3 (+), Mamoglobin (+), ER (+), PR (+), MUC2 (-), Synaptophysin (-), and Chromogranin (-) in tumor cells. Morphological and IHC findings were evaluated together, leading to the interpretation favoring metastasis from primary breast carcinoma. Post-operative 18F-FDG and 68Ga-FAPI PET/CT imaging revealed that the primary tumor in the left breast did not show significant 18F-FDG uptake (SUVmax: 1.9) but exhibited mild focal 68Ga-FAPI uptake (SUVmax: 3.1).

In a patient with a ductal subtype, magnetic resonance imaging (MRI) revealed satellite lesions suggestive of ductal carcinoma in situ (DCIS) in the retroareolar region. The corresponding areas showed mild 18F-FDG uptake on PET/CT imaging. In all patients, both radiological imaging and FDG PET/CT did not reveal any evidence supporting an inflammatory carcinoma pattern consistent with the histopathological findings. The uptake of all primary lesions described in

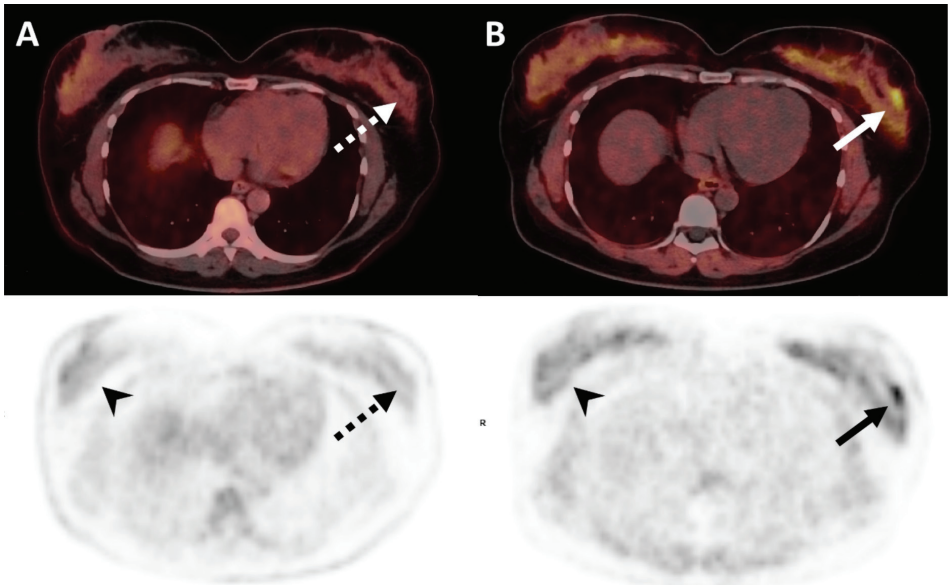

Figure 2. A, 18F-FDG PET/CT: 18F-Fluorodeoxyglucose Positron Emission Tomography/Computed Tomography images. The dashed arrow indicates the primary tumor. **B,** 68Ga-FAPI PET/CT: 68Gallium-Fibroblast activation protein inhibitor images. Arrow depicts uptake in the primary tumor. Arrowheads indicate background parenchymal uptake.

both PET/CT studies and additional PET/CT findings were histopathologically confirmed.

According to the analysis results, only a strong positive correlation was found between the primary tumor SUVmax value and the Ki67% index (r=+0,747, p=0,002) (Figure 3). No correlation was found between other variables (age, molecular subtype, nuclear grade, estrogen/progesterone receptor score and percentage, HER-2 score, primary tumor size, axillary lymph node size, and SUVmax) and the primary tumor SUVmax (p>0,05).

Axillary lymph node metastasis was confirmed histopathologically in 64% (n=9) of the patients enrolled in the study. Specifically, among the patients, lymph node metastases were observed in five patients (100%) classified as ductal carcinoma and four patients (44%) with lobular subtypes. In all these patients, increased 18F-FDG uptake was detected in the lymph nodes on PET/CT (mean SUVmax=10.9±16.0; size=10–60 mm) (Table 3).

In one patient, 18F-FDG PET/CT demonstrated additional intra-abdominal lymph nodes and bone metastases. In this patient, bone and lymph node metastases were generally stable during the most recent 18F-FDG PET/CT follow-up conducted at the 60th month. In another patient, in addition to the intense 18F-FDG uptake in the primary breast tumor, widespread, high 18F-FDG uptake was detected in multiple bone metastases. Moreover, a hypermetabolic lymph node in the supraclavicular region and the ipsilateral axillary lymph nodes were also detected. The 18F-FDG PET/CT imaging conducted for treatment response assessment revealed metabolic regression in the primary tumor, lymph nodes, and bone metastases.

In follow-up, two of the patients have passed away. In one patient, 18F-FDG PET/CT demonstrated intense FDG uptake in cervical, mediastinal, and contralateral axillary lymph nodes, along with the primary tumor and axillary lymph nodes. At the third-year follow-up, disease progression was detected, and the patient died. In another patient, in the staging PET/CT imaging, only the primary tumor showed mild 18F-FDG uptake, and no locoregional or distant metastases were detected. However, bone metastases were observed on the 36th-month follow-up 18F-FDG PET/CT imaging. Subsequently, disease progression was detected in the liver during follow-up, and the patient passed away in the 59th month.

In the Kaplan-Meier survival analysis, median survival could not be reached in both groups, and the

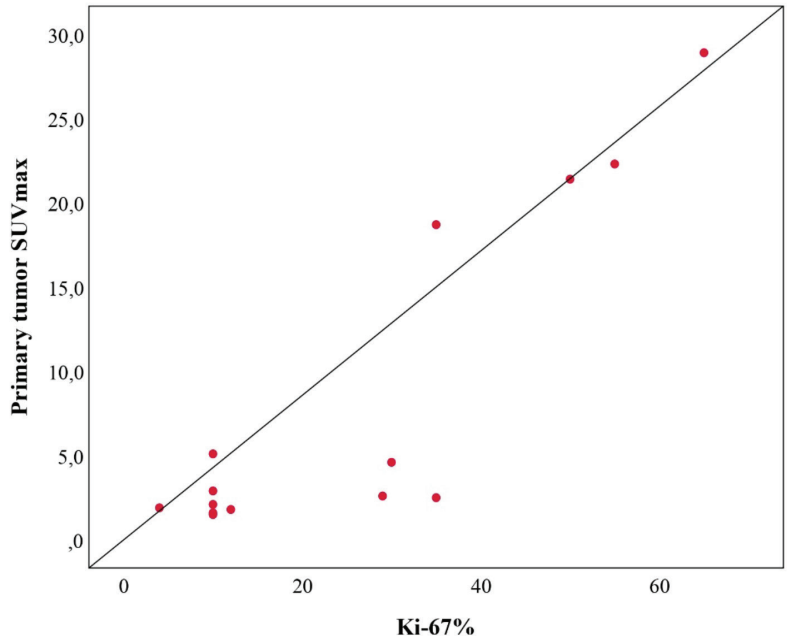

Figure 3. The positive correlation between the primary tumor SUVmax value and the Ki67% index.

mean overall survival was determined as 92.8 ± 7.7 months (95% CI 77.5–108.0). Furthermore, in the subgroup analysis, the mean overall survival for the lobular group was calculated as 98.4 ± 6.0 months (95% CI 86.5–110.3), while for the ductal group, it was 54.3 ± 7.8 months (95% CI 38.8–69.8). The two groups did not have significant statistical differences in the overall comparison (Log Rank, Chi-Square=1.035, p=0.309).

DISCUSSION AND CONCLUSION

Our study has identified significant 18F-FDG uptake in cases of ductal carcinoma with SRC differentiation, despite the widely accepted notion that SRCC exhibits low affinity for 18F-FDG. Additionally, in cases of lobular carcinoma with SRC differentiation, considering alternative PET radiopharmaceuticals in addition to 18F-FDG may be prudent, as 18F-FDG's low affinity might compromise the staging accuracy.

In breast cancer, molecular subtypes are crucial in tailoring personalized patient treatment. In the study conducted by Zheng et al., which investigated the clinicopathological and IHC characteristics of breast carcinomas with SRC differentiation, it was reported that all patients had positive ER expression, variable PR expression, and negative HER2 expression. Additionally, the average Ki-67% value was 20 (10). In the study by Ohashi et al., 22 patients with signet-ring cell breast cancer were evaluated, of whom 15 patients were ER-positive, 12 patients were PR-positive, and HER-2 positivity was observed in only 1 case, the mean Ki-67% was 13 (7). In the study conducted by Akin et al., 25 patients were examined, and ER (76%), PR (56%), and HER-2 (28%) positivity were detected (11). In our study, ER was positive in almost all patients, and Ki-67% scores were similar to previous findings. Furthermore, HER-2 positivity was observed in 4 patients, and one patient was identified as having the HER-2 molecular subtype.

18F-FDG uptake can provide valuable information on the staging and metabolic activity of the tumor, which can help determine the aggressiveness of the disease and guide therapy decisions, including breast cancer with SRC differentiation. High uptake of 18F-FDG is associated with aggressive features of cancer cells and poor prognosis (12,13). However, the specific relationship between 18F-FDG uptake and breast cancer with SRC differentiation has not been extensively studied. In the literature, a few case studies have shown the association between 18F-FDG uptake and this rare type of cancer. In the case reported by Parihar et al., SRC differentiation was observed along

with mucinous carcinoma. Both the primary tumor and metastases demonstrated low 18F-FDG affinity, consistent with the nature of mucinous tumors, which exhibit high extracellular mucin and low cellular components (14). In the study by Lebron et al., a case of moderately differentiated, estrogen receptor-positive lobular carcinoma with signet ring cell features was reported. In 18F-FDG PET/CT imaging, minimal FDG uptake was noted in the breast masses, axillary lymph node, and sclerotic lesions observed in the spine (15). In another case, gastric metastasis of SRC differentiated breast cancer at follow-up did not show pathological 18F-FDG uptake (16). Our study observed higher 18F-FDG uptake in patients with SRC differentiated ductal carcinoma than those with lobular carcinoma. This finding might be associated with higher grade and Ki-67% values in the ductal cases. Additionally, we identified only Luminal B and HER-2 molecular subtypes in the ductal group, while most of the lobular group consisted of the Luminal A subtype.

In some cases, SRC-differentiated breast cancer has been demonstrated using radiopharmaceuticals other than 18F-FDG. In the case presented by Parihar et al., in addition to 18F-FDG, 68Ga-PSMA PET/CT imaging was performed for the patient. 68Ga-PSMA showed higher uptake in the primary tumor and metastatic lesions compared to 18F-FDG. This might be attributed to PSMA expression affecting vascular endothelial cells rather than tumor cells and highlights the potential of 68Ga-PSMA as an alternative method for better characterization, especially in cancers with known low FDG avidity, such as mucinous malignancies (14). In another case of breast cancer with stomach and bone metastases, Tc-99m MIBI scintimammography demonstrated bilateral breast cancer with SRC differentiated lobular carcinoma (17). In the case report by Li et al., metastases originating from mixed invasive ductal-lobular breast cancer in the gastric, peritoneal, and ovarian regions were reported to exhibit low-level uptake on 18F-FDG PET/CT. However, on 68Ga-FAPI PET/CT, higher uptake levels were observed. They also emphasized that 68Ga-FAPI PET/CT may offer significant advantages in such cases, as false-negative results may occur in malignant lesions with inactive glucose metabolism, such as SRCC and mucinous tumors, in 18F-FDG PET/CT (18). In our study, an additional 68Ga-FAPI imaging was performed on two patients with lobular carcinoma, and similar to the previous case studies, superior results were observed compared to 18F-FDG in these two patients as well.

Recent studies have indicated that 18F-FDG PET/CT may not be as effective as 68Ga-FAPI-04 PET/CT in detecting SRCCs that originate from certain organs other than the breast (19-23). In the study conducted by Pang et al., which involved 35 patients with gastric, duodenal, and colorectal cancer, nine patients were diagnosed with SRCC. The study findings indicated that 68Ga-FAPI PET/CT demonstrated higher tracer uptake and sensitivity than 18F-FDG PET/CT in primary lesions, lymph nodes, bone, and visceral metastases (19). In a multicenter study conducted by Chen et al., representing the most extensive series comparing 18F-FDG and 68Ga-FAPI in gastric SRCC, FAPI PET demonstrated higher radiotracer uptake, tumor-to-background ratios, and diagnostic accuracy compared to 18F-FDG PET in the detection of primary/recurrent tumors and metastatic lesions (23). In the study performed by Lin et al., comparing cases of colorectal cancer, eight patients with mucinous/SRCC were reported. The study suggested that Ga-FAPI-04 PET/CT could be a useful imaging method for detecting and staging SRCC/mucinous carcinomas in patients with colorectal cancer (20). In the comprehensive study of Hirmas et al., which included 21 tumor entities, one patient with pancreatic SRCC was reported. The study demonstrated that 68Ga-FAPI showed increased absolute uptake and higher tumor-to-background uptake, resulting in improved tumor detection in cases of pancreatic cancer (21). Additionally, in a case study conducted at our clinic, intense uptake was reported in prostatic SRCC and its metastases on 68Ga-FAPI PET/CT, highlighting the efficacy of 68Ga-FAPI-04 imaging in detecting tumor and bone metastases in primary prostate SRCC (22). The results of these studies indicate that in cancer cases involving SRC differentiation, 68Ga-FAPI may yield more successful outcomes than 18F-FDG. Based on our findings, our study observed that, in the context of breast cancer, only lobular cancers exhibited low 18F-FDG uptake patterns, similar to other SRCCs.

Numerous valuable studies have investigated the relationship between SUVmax of primary breast can-

cer and its histopathology, IHC, and survival characteristics. In our study, the higher 18F-FDG uptake in metastatic lymph nodes is more prominent in the ductal group with higher-grade and more aggressive IHC findings. Furthermore, the statistically significant correlation found only between primary tumor SUVmax and Ki-67% can be considered a limitation of the study, given the rarity of this subtype, as it pertains to a cohort of only 14 patients.

In cases where SRCs are identified in a breast specimen, evaluating specific IHC features is crucial to differentiate between primary and metastatic lesions. Differentiating between breast SRCC and gastrointestinal SRCC is crucial for managing patients and can eliminate unnecessary treatments. Cases have been reported indicating the metastasis of gastrointestinal SRCC, mainly originating from the stomach to the breast, as well as the metastasis of breast SRCC to the gastrointestinal system (24-27). IHC staining can be a valuable tool for distinguishing between breast and gastrointestinal SRCC. In the study by Hui et al., it was reported that ER, GATA-3, CK20, and CDX2 were expressed at varying levels in SRCCs originating from the breast and gastrointestinal sources. These markers were noted to exhibit superior characteristics in distinguishing the respective tumors (28). PET/CT plays a vital role in managing patients with histopathological diagnosis of SRCC by determining whether the breast lesion is a primary tumor or SRCC metastasis from other sites (9).

The study by Wang et al. compared survival outcomes of 167 patients with Primary breast SRCC and 11,648 patients with Mucinous breast cancer. The analysis results indicated that patients with SRCC exhibited more aggressive histopathological characteristics and had lower overall survival (OS) and breast cancer-specific survival (BCSS) than patients with MBC. Despite being reported as a more aggressive subtype of breast cancer compared to MBC, breast cancers with SRC differentiation have demonstrated better OS than SRCCs originating from other organs (29). In Wu et al.'s SEER database study, all cases of SRCC were examined. A 5-year OS of 69% was reported for breast-originating SRCC, whereas the most commonly observed gastric SRCC showed a 5-year survival rate of 22%. For SRCC originating from other organs such as the esophagus, lung, pancreas, and gallbladder, the 5-year survival was reported to be below 15%. Additionally, it was noted that survival in breast-originating SRCC remains dependent on the tumor stage at the time of diagnosis (4). In the study conducted by Wang et al. evaluating primary breast SRCCs, the 5-year overall survival rate was reported as 73.7%, the 5-year relapse-free survival rate was 54.3%, and the 5-year breast cancer-specific survival rate was 78.3% (30). Similar OS results were obtained in our study, which was conducted with a limited number of patients.

This study has some limitations. Firstly, due to the rarity of this specific subtype of breast cancer, our retrospective analysis was conducted within a single center and involved a restricted number of patients. This constrained patient pool may impact the generalizability of our findings. Furthermore, the inherent nature of the limited sample size could potentially compromise the strength and reliability of our conclusions, particularly in the assessment of long-term outcomes like survival and various other parameters.

In conclusion, to the best of our knowledge, there is currently a lack of studies that have assessed the clinical characteristics of breast cancer subtypes specifically related to SRC differentiation using 18F-FDG PET/CT imaging. The uptake of 18F-FDG was significantly higher in the ductal type compared to the lobular type. Due to the low 18F-FDG uptake detected in lobular carcinoma with SRC differentiation, further studies with alternative PET radiopharmaceuticals such as FAPI and PSMA may be recommended in this patient group.

Conflict-of-interest and financial disclosure

The authors declare that they have no conflict of interest to disclose. The authors also declare that they did not receive any financial support for the study.

REFERENCES

1. Siegel RL, Miller KD, Wagle NS, Jemal A. Cancer statistics, 2023. CA Cancer J Clin. 2023;73(1):17-48.
2. Lakhani SR, Ellis IO, *WHO classification of tumours of the breast*. 4th ed. IARC; 2012.
3. Chu PG, Weiss LM. Immunohistochemical characterization of signet-ring cell carcinomas of the stomach,

breast, and colon. Am J Clin Pathol. 2004;121(6):884-92.
4. Wu SG, Chen XT, Zhang WW, et al. Survival in signet ring cell carcinoma varies based on primary tumor location: a surveillance, epidemiology, and end results database analysis. Expert Rev Gastroenterol Hepatol. 2018;12(2):209-14.
5. Saphir O. Signet-ring cell carcinoma. Mil Surg. 1951;109(4):360-9.
6. Merino MJ, Livolsi VA. Signet ring carcinoma of the female breast: A clinicopathologic analysis of 24 cases. Cancer. 1981;48(8):1830-7.
7. Ohashi R, Hayama A, Yanagihara K, et al. Prognostic significance of mucin expression profiles in breast carcinoma with signet ring cells: a clinicopathological study. Diagn Pathol. 2016;11(1):131.
8. Sinn HP, Kreipe H. A brief overview of the WHO classification of breast tumors, 4th edition, focusing on issues and updates from the 3rd edition. Breast Care (Basel). 2013;8(2):149-54.
9. Li X, Feng YF, Wei WD, et al. Signet-ring cell carcinoma of the breast: a case report. World J Surg Oncol. 2013;11(1):183.
10. Zheng J, Liu J, Yang W, Yao J, Guo J, Liu C. The clinicopathological and immunohistochemical features of breast carcinomas with signet-ring-cell differentiation. World J Surg Oncol. 2023;21(1):181.
11. Akin S, Diker O, Kertmen N, et al. Signet ring cell carcinoma of breast: Single center experience. J Clin Oncol. 2015;33(15_suppl):e11513-e.
12. Buck A, Schirrmeister H, Kuhn T, et al. FDG uptake in breast cancer: correlation with biological and clinical prognostic parameters. Eur J Nucl Med Mol Imaging. 2002;29(10):1317-23.
13. Alçin G, Arslan E, Aksoy T, Akbas S, Cermik TF. FDG uptake in breast cancer and quantitative assessment of breast parenchymal uptake on 18F-FDG PET/CT: association with histopathological, hormonal status, and clinical features. Int J Radiat Res. 2022;20(4):815-21.
14. Parihar AS, Mittal BR, Sood A, Basher RK, Singh G. 68Ga-prostate-specific membrane antigen PET/CT and 18F-FDG PET/CT of primary signet ring cell breast adenocarcinoma. Clin Nucl Med. 2018;43(11):e414-e6.
15. Lebron L, Greenspan D, Pandit-Taskar N. PET imaging of breast cancer: role in patient management. PET Clin. 2015;10(2):159-95.
16. Hara F, Kiyoto S, Takabatake D, et al. Metastatic breast cancer to the stomach resembling early gastric cancer. Case Rep Oncol. 2010;3(2):142-7.
17. Park CH, Whang HS, Park HB. Bilateral signet-ring cell carcinoma of the breast: scintigraphic findings. Clin Nucl Med. 1996;21(2):115-7.
18. Li T, Jiang X, Zhang Z, et al. Case Report: (68)Ga-FAPI PET/CT, a more advantageous detection mean of gastric, peritoneal, and ovarian metastases from breast cancer. Front Oncol. 2022;12:1013066.
19. Pang Y, Zhao L, Luo Z, et al. Comparison of (68)Ga-FAPI and (18)F-FDG uptake in gastric, duodenal, and colorectal cancers. Radiology. 2021;298(2):393-402.
20. Lin X, Li Y, Wang S, et al. Diagnostic value of [(68)Ga]Ga-FAPI-04 in patients with colorectal cancer in comparison with [(18)F]F-FDG PET/CT. Front Oncol. 2022;12:1087792.
21. Hirmas N, Hamacher R, Sraieb M, et al. Fibroblast-activation protein PET and histopathology in a single-center database of 324 patients and 21 tumor entities. J Nucl Med. 2023;64(5):711-6.
22. Tatar G, Baykal Koca S, Sevindir I, Ergul N, Cermik TF. 68 Ga-FAPI-04 PET/CT ın primary signet ring-like cell carcinoma of prostate with bone metastases. Clin Nucl Med. 2023;48(4):e188-e9.
23. Chen H, Pang Y, Li J, et al. Comparison of [(68)Ga]Ga-FAPI and [(18)F]FDG uptake in patients with gastric signet-ring-cell carcinoma: a multicenter retrospective study. Eur Radiol. 2023;33(2):1329-41.
24. Avgerinou G, Flessas I, Hatziolou E, et al. Cutaneous metastasis of signet-ring gastric adenocarcinoma to the breast with unusual clinicopathological features. Anticancer Res. 2011;31(6):2373-8.
25. Ben Kridis W, Lajnef M, Fki A, Belaid L, Khanfir A. An uncommon case of synchronous gastric and colonic metastases from breast cancer. JGH Open. 2022;6(8):587-9.
26. Sato T, Muto I, Hasegawa M, et al. Breast signet-ring cell lobular carcinoma presenting with duodenal obstruction and acute pancreatitis. Asian J Surg. 2007;30(3):220-3.
27. Zhang L, Wu L, Li J, et al. Gastrointestinal metastatic signet ring cell breast cancer in young females: a case report. Gland Surg. 2022;11(5):943-52.
28. Hui Y, Wang Y, Nam G, et al. Differentiating breast carcinoma with signet ring features from gastrointestinal signet ring carcinoma: assessment of immunohistochemical markers. Hum Pathol. 2018;77:11-9.
29. Wang S, Zhang Y, Yin F, Zhang X, Yang Z, Wang X. Prognostic analysis of primary breast signet ring cell carcinoma and mucinous breast adenocarcinoma: A SEER population-based study. Front Oncol. 2021;11:783631.
30. Wang T, Shen B, Wang L, Liu F. Primary signet ring cell carcinoma of the breast: A rare entity with unique biological behavior-A clinical study based on pure signet ring cell carcinoma cohort. Pathol Res Pract. 2020;216(6):152948.